

MiR-1301-3p Inhibits Epithelial to Mesenchymal Transition via Targeting RhoA in Pancreatic Cancer

Xinxue Zhang (✉ 790344705@qq.com)

Beijing Chao-Yang Hospital: Beijing Chaoyang Hospital <https://orcid.org/0000-0002-8900-1688>

Xin Zhao

Beijing Chao-Yang Hospital: Beijing Chaoyang Hospital

Junming Xu

Beijing Chao-Yang Hospital: Beijing Chaoyang Hospital

Jun Ma

Beijing Chao-Yang Hospital: Beijing Chaoyang Hospital

Zhe Liu

Beijing Chao-Yang Hospital: Beijing Chaoyang Hospital

Jiantao Kou

Beijing Chao-Yang Hospital: Beijing Chaoyang Hospital

Ren Lang

Beijing Chao-Yang Hospital: Beijing Chaoyang Hospital

Qiang He

Beijing Chao-Yang Hospital: Beijing Chaoyang Hospital

Research

Keywords: miR-1301-3p, RhoA, EMT, pancreatic cancer

Posted Date: September 17th, 2020

DOI: <https://doi.org/10.21203/rs.3.rs-76083/v1>

License:  This work is licensed under a Creative Commons Attribution 4.0 International License.

[Read Full License](#)

Version of Record: A version of this preprint was published at Journal of Oncology on February 26th, 2022. See the published version at <https://doi.org/10.1155/2022/5514715>.

Abstract

Background: Micro(mi)RNAs play an essential role in the epithelial-mesenchymal transition (EMT) process in human cancers. This study aimed to uncover the regulatory mechanism of miR-1301-3p on EMT in pancreatic cancer (PC).

Methods: GEO database (GSE31568, GSE41372, and GSE32688) and the PC cohort of The Cancer Genome Atlas were applied to discover the expression and prognostic role of miR-1301-3p. In the validation cohort, qRT-PCR was performed in 72 paired PC tissue samples. CCK-8, wound healing, and transwell migration assays were used to detect miR-1301-3p function on PC cells. Luciferase reporter assays and western blotting were performed to discover the potential target of miR-1301-3p on EMT.

Results: Our study revealed that miR-1301-3p was downregulated in PC tissues compared with normal samples. A low level of miR-1301-3p was associated with malignant pathological differentiation, lymphatic metastasis, tumor residual, and unsatisfactory overall survival. Gene Ontology analyses indicated that miR-1301-3p possibly regulated cell cycle and adheren junction. *In vitro* assays showed that miR-1301-3p suppressed proliferation, migration, and invasion ability of PC cells. Mechanically, miR-1301-3p inhibits RhoA expression, and knockdown of RhoA upregulated E-cadherin; however, downregulated N-cadherin and vimentin level.

Conclusions: MiR-1301-3p acts as a prognostic biomarker for PC and inhibits PC progression by targeting RhoA induced EMT process.

Introduction

Pancreatic cancer (PC) is the fourth leading cause of cancer-related deaths worldwide. Recently, surgical techniques and drug therapies for PC developed certainly. However, the long-term outcome of pancreatic cancer is still low, with a 5-year overall survival (OS) of 5%^[1]. There were no symptoms and specific biomarkers in the early stage of pancreatic cancer. Consequently, most patients were diagnosed with PC at an advanced stage and lost the opportunity for radical operation^[2].

As a small non-coding RNA, micro(mi)RNA degrades mRNA by targeting 3'-untranslated region (3'-UTR). Accumulating studies have revealed that miRNAs regulate multiple cellular biological processes such as proliferation^[3], differentiation^[4], apoptosis^[5], and epithelial-mesenchymal transition (EMT)^[6]. In breast cancer and glioma, miR-1301-3p inhibits cell proliferation via downregulating ICT1 and N-RAS, respectively^[7, 8]. In our previous study, miR-1301-3p was low expressed in PC samples compared with healthy tissues, and a high-level of miR-1301-3p was associated with good OS^[9]. Therefore, it is worth investigating the potential functions and mechanisms of miR-1301-3p in PC progression.

In this study, we demonstrated that miR-1301-3p served as a prognostic biomarker for PC and inhibited RhoA (Ras homologue family member A) induced EMT process.

Materials And Methods

Differential and survival analyses for miR-1301-3p

We extracted miR-1301-3p expression data from three PC-miRNA expression profiles (GSE31568, GSE41372, and GSE32688) of the Gene Expression Omnibus (GEO) database. Next, we compared the difference of miR-1301-3p between PC sample tissues and healthy tissues. To verify the prognostic importance, the clinical data and miR-1301-3p expression value were also obtained based on the PC cohort of The Cancer Genome Atlas (TCGA) database. According to the median value of miR-1301-3p, we divided the PC patients into high and low-level groups and performed Kaplan-Meier survival analyses. A *P*-value was calculated by the log-rank test.

Patients and samples in the validation cohort

Between February 2018 and August 2020, a total of 72 PC patients were enrolled in the validation cohort, who were admitted to the Department of Hepatobiliary Surgery in Beijing Chao-Yang Hospital. These patients had not accepted radiotherapy or chemotherapy preoperatively, and the final diagnosis was determined by pathological results. Paired PC sample tissues and adjacent normal tissues were immediately stored in liquid nitrogen for two hours and then transferred into -80°C refrigerator for storage. Postoperatively, these patients have followed an average of 12 months, ranging from two to 29 months. The ethics committee of Beijing Chao-Yang Hospital approved this study, and all the patients signed the informed consent form.

Function annotation and signaling pathway enrichment for miR-1301-3p

We first applied the miRWalk2.0 database to predict the binding genes of miR-1301-3p and then performed correlation analyses between mRNA expression of these genes and miR-1301-3p value based on the PC cohort of TCGA. Finally, the combinative genes negatively correlated with miR-1301-3p were regarded as the target genes of miR-1301-3p.

To understand the functions of these target genes, we performed Gene Ontology (GO) and Kyoto Encyclopedia of Genes and Genomes (KEGG) pathway enrichment analyses using the clusterProfiler R package^[10]. A protein-protein interaction (PPI) network was constructed using the Search Tool for the Retrieval of Interacting Genes database and visualized with Cytoscape software. The correlation of each PPI relationship pair was represented by a combined score ranging from 0 (low) to 1 (high). In our study, an interaction > 0.4 (moderate) was applied as the cut-off value. The Molecular Complex Detection plug-in in Cytoscape software was used to identify the hub genes among the PPI network. The screening conditions were set as degree cut-off = 2, K-Core = 2, and Node Score Cutoff = 0.2. Besides, we verified the hub gene expression using the PC-mRNA data of GSE16515.

Quantitative real-time polymerase chain reaction

TRIzol (Invitrogen, USA) was used for total RNA extraction and qualified using the NanoDrop ND-1000 (Thermo Fisher, USA). Total RNA was converted to first-strand cDNA according to the manufacturer's protocol (rtStar™ First Strand cDNA Synthesis Kit, Arraystar Inc.). Specific primers for miR-1301-3p was designed by RiboBio (Guangzhou, China). The sequence of forward and reverse primers for miR-1301-3p was 5'-ACACTCCAGCTGGGTTCAGCTGCCTGGGAGT-3' and 5'-CTCAACTGGTGTCTGGAGTCGGCAATTCAGTTGAGGAAGTCAC-3'. qRT-PCR was performed using Arraystar SYBR® Green Real-time qPCR Master Mix (Arraystar Inc) according to the manufacturer's instruction. The relative expression of miR-1301-3p was calculated using the $2^{-\Delta\Delta Ct}$ method and normalized to β -actin expression levels.

Cell culture and transfection

Five PC cell lines were selected to test the expression of miR1301-3p, including SW1990, AsPC-1, CFPAC-1, PANC-1, and Patu-8988. These cells were purchased from the American Type Culture Collection (Manassas, VA, USA). We cultured the PC cells with DMEM medium (Biological Industries) containing penicillin/streptomycin and 10% fetal bovine serum (FBS) at 37 °C with 5% CO₂. Since miR-1301-3p high expressed in SW1990 and PANC-1 cells (Fig. 2A), we selected these two cell lines to conduct further experiments.

MiR1301-3p mimics, inhibitor, and negative control (NC) were designed and synthesized by RiboBio (Guangzhou, China). Small interference RNA against RhoA (si-RhoA)-535, 575, and 628 were designed and synthesized by GenePharma (Shanghai, China). In brief, miR-1301-3p mimics and inhibitor (100 nM) were transfected into PANC-1 and SW1990 cells, using Lipofectamine 3000 reagent (Invitrogen, USA), following the manufacturer's instruction.

Cell Counting Kit-8 (CCK-8) assays

According to the manufacturer's instruction, we performed CCK-8 assays (Sigma, Aldrich) to examine the proliferation ability of PC cells. Approximately 2×10^3 cells were added to each well of the 96-well plate, and then, the plate was cultured for 24 h at 37 °C. Next, we added 50 μ l of the miR-1301-3p mimics, inhibitor, and NC to wells of the 96-well plate. Then the plate was placed in the 37 °C incubator again for 24 h. At 0, 24, 48, 72, and 96 h, 10 μ l CCK-8 solution was added into each well. After 2 h, optical density (OD) 450 nm values were measured using the enzyme-labeled instrument (Bio-Rad, United States). Cells were tested three times for each group.

Transwell migration and invasion assays

We conducted transwell migration assays with a 6.5 chamber with 8 μ m pores (Corning, NY, USA). A suspension containing 1×10^4 PANC-1 and SW1990 cells were prepared and suspended separately in serum-free DMEM and added into the upper chamber. After that, 500 μ l of 10% serum-containing DMEM was added into the lower chamber of the well and incubated 24 h at 37 °C. After 24 h, PC cells in the upper chamber were removed. For transwell invasion assays, 1×10^4 cells were seeded on the Matrigel-coated membrane inserts. We used 0.1% crystal violet to stain the cells that migrated into the underside

of the membrane. Four random fields were selected at 4 × magnification for counting cell numbers. Each experiment was performed three times.

Wound healing assays

SW1990 and PANC-1 cells (1×10^5) were incubated in six-well culture plates for 48 h until the cells were 80–90% confluent. Cells were maintained in 10% FBS containing DMEM media for 24 hours. PBS was used to wash away the non-adherent cells. A sterile 200- μ l pipet was used to make a scratch in the center of the cell monolayer. The monolayer was washed three times with PBS, and fresh media was added. After 0 h, 24 h, and 48 h, the wound width was measured at 2.5 × magnification. Each assay was performed three times.

Protein extraction and western blotting assays

Total protein was extracted from PC cells after 72 h transfection, and the BCA protein assay kit (Beyotime, China) was used to measure protein concentration followed by the manufacturer's instruction. Briefly, 12% SDS-PAGE was used for electrophoresis, and then the proteins were transferred to PVDF membranes. Glyceraldehyde-3-Phosphate Dehydrogenase (GAPDH), RhoA, E-cadherin, N-cadherin, and Vimentin antibodies were used to analyze total protein. Specific primary rabbit-anti-human antibodies (CST, 1:1000) were used to incubate the membranes at 4 °C overnight. On the second day, the membranes were incubated with HRP-conjugated anti-rabbit IgG antibodies (1:2000) at room temperature for 1 h. An enhanced chemiluminescence detection system was used to visualize the bands. GAPDH was used as an internal control. Rabbit anti-GAPDH, RHOA, N-cadherin, E-cadherin, and vimentin antibodies (Cell Signaling Technology, Danvers, MA, USA) were used to analyze cell lysates.

Luciferase reporter assays

According to starBase network tool, RhoA is a predicted target for miR1301-3p. The binding site between miR1301-3p and 3'UTR of RhoA was evaluated by using the pmirGLO dual-luciferase miRNA expression vector containing wild type (WT) or mutant (MUT) 3'UTR of RhoA. The WT or MUT 3'UTR of RhoA and miR-1301-3p mimics were co-transfected into PANC-1 cells. After 48 h, the luciferase reporter assay system was used to examine the luciferase activity. Each experiment was performed in triplicate.

Statistical analysis

R software version 3.6.0 was used to perform statistical analyses. Continuous variables between the two groups were compared by a paired sample *t*-test. The data were presented as the mean \pm standard deviation. Qualitative data were analyzed by the chi-square test. Fisher's exact test was employed to compare the categorical variables among groups. GraphPad Prism 8.0 (GraphPad Software, Inc. La Jolla, CA, USA) was applied to produce figures. *P*-value < 0.05 was considered statistically significant.

Results

MiR-1301-3p was downregulated in PC tissues and correlated with prognosis

Based on miRNA microarray data (GSE31568, GSE 41372, GSE32688), miR1301-3p was significantly downregulated in PC tissues, compared with normal tissues (Fig. 1A-C; $p < 0.05$). In our validated cohort, including 72 pairs of PC and adjacent healthy tissues, the miR1301-3p level was higher in tumor samples than healthy samples (Fig. 1D; $p < 0.001$). Furthermore, a high level of miR1301-3p was associated with good OS in the PC cohort of TCGA (Fig. 1E; $p < 0.0054$). Similarly, the OS was significantly longer in the high-level group than in the low-level group for the validated cohort (Fig. 1F; $p < 0.0047$). The univariate analyses showed that a low-level of miR1301-3p related to malignant pathological differentiation, tumor residual, and lymphatic metastasis in PC patients (Table 1). Nevertheless, there was no statistical significance with age, gender, tumor size, vascular invasion, TNM stage, primary tumor stage, lymph node invasion, and distance metastases.

Table 1
Association between miR-1301-3p level and the clinicopathological parameters of pancreatic cancer patients in the study cohort.

Clinical parameters	miR-1301-3p		P. Value
	Low(n = 36)	High(n = 36)	
Age (years)	61	64	0.327
Gender			0.637
Male	21	18	
Female	15	18	
Pathological differentiation			< 0.001
Moderate and high	18	33	
Poor	18	3	
Tumor size (cm)	4.0 ± 1.5	3.7 ± 2.1	0.608
Resection			0.018
R0	24	33	
R1 and R2	12	3	
Numbers of positive lymph node	5.0 ± 4.5	1.5 ± 1.8	< 0.001
Vascular invasion			0.634
Negative	19	22	
Postitive	17	14	
TNM stage			0.285
I and IIA	7	12	
IIB and IV	29	24	
Primary tumor			0.443
T1 and T2	23	27	
T3 and T4	13	9	
Reginal lymph nodes			0.119
N0	7	14	
N1 and N2	29	22	
Distant metastases			0.107

Clinical parameters	miR-1301-3p		P. Value
Negative	30	35	
Postitive	6	1	

MiR-1301-3p inhibited proliferation, migration, and invasion abilities of pancreatic cancer cells

As shown in Fig. 2A, the miR-1301-3p level was relatively high in SW1990 and PANC-1 cells among five PC cell lines. Thus, we used SW1990 and PANC-1 cells to perform *in vitro* experiments. CCK-8 assays showed that miR-1301-3p mimics significantly suppressed PC cell proliferation (Fig. 2B). Wound healing and transwell migration assays demonstrated that the migration ability of PC cells was lower in miR-1301-3p mimics group than that in the NC group (Fig. 2C and Fig. 3). Similarly, the invasion ability of SW1990 and PANC-1 cells were also downregulated, transfected with miR-1301-3p mimics (Fig. 3).

GO annotation and KEGG pathway enrichment for MiR-1301-3p

The GO analyses showed that the target genes of miR-1301-3p were enriched in positive regulation of cell cycle, TGF- β receptor signaling pathway, and cellular response to TGF- β stimulus in biological process (Fig. 4A). The following cellular components were largely enriched in adherens junction, focal adhesion, and cell-substrate junction (Fig. 4B). Finally, the following molecular functions were mostly enriched in anion transmembrane transporter activity and guanyl nucleotide binding (Fig. 4C). The KEGG pathway analyses displayed that the target genes of miR-1301-3p were mainly enriched in the phospholipase D signaling pathway and Ras signaling pathway (Fig. 4E). These results suggested that miR-1301-3p was associated with cell migration and PC development.

MiR-1301-3p inhibits RhoA

In the PPI network, we identified 11 hub genes associated with miR-1301-3p, and among them, RhoA served as a central gene (Fig. 5A). As shown in Fig. 5B, miR miR-1301-3p negatively correlated with RhoA expression in the PC cohort of TCGA. Through the starBase network tool, the binding site was identified between miR-1301-3p and RhoA 3'UTR (Fig. 5C). After that, luciferase reporter assays showed that miR-1301-3p mimics significantly downregulated the relative luciferase activity of RhoA-WT in PANC-1 cells (Fig. 5C). In PANC-1 and SW1990 cells, miR-1301-3p mimics decreased RhoA protein expression, while miR-1301-3p inhibitor increased RhoA level (Fig. 5D). Collectedly, these results support that miR-1301-3p suppresses RhoA expression.

RhoA silencing inhibited the EMT process in PC cells

Three small interference RNAs were separately transfected into PANC-1 cells to knockdown RhoA expression, including si-RhoA-535, 575, and 628 (Fig. 6A). The results suggested that RhoA levels decreased significantly, and then we selected si-RhoA-535 for RhoA inhibition.

In PC cells, N-cadherin and vimentin protein expressions were lower in the si-RhoA transfecting group than those in the NC group. However, E-cadherin was upregulated after the transfection of si-RhoA. On the contrary, the vimentin level was higher in the RhoA-knockdown group than in the NC group. Taken together, these results suggested that RhoA suppression inhibited EMT proteins in PC cells.

Discussion

Recent studies demonstrated that miR-1301-3p functioned as a tumor suppressor in multiple human cancer cells^[11]. For example, miR-1301-3p inhibited Wnt/ β -catenin signaling pathway through targeting BCL9 in hepatocellular carcinoma^[12]. Similarly, NNT-AS1 promoted bladder cancer cell proliferation by targeting miR-1301-3p/PODXL axis and activating Wnt pathway^[13]. Besides, ABHD11-AS1 and LINC01433 upregulated STAT3 level by sponging miR-1301-3p and promoted tumor progression in papillary thyroid carcinoma and hepatocellular carcinoma, respectively^[14, 15]. Hence, the function of miR-1301-3p is needed to elucidate for pancreatic cancer.

GO term of biological process revealed that five target genes of miR-1301-3p were enriched in “positive regulation of cell cycle,” which indicated that miR-1301-3p suppressed cancer cell proliferation through negatively regulating cell cycle. Moreover, the target genes of miR-1301-3p were mostly enriched in cell junction for the other GO terms of cellular component and molecular function, which suggested that this microRNA could affect cell migration by regulating cell adhesion. In KEGG analyses, the target genes of miR-1301-3p were enriched in “Ras signaling pathway,” “phospholipase D signaling pathway,” and “microRNAs in cancer” pathway. Collectively, miR-1301-3p may exert tumor-suppressive functions via regulating cell cycle, cell junction, and cancer-associated pathways. Inspired by these signaling pathways, to our knowledge, we first provide evidence that miR-1301-3p directly targets RhoA and suppresses the EMT process in pancreatic cancer.

In this study, GEO and our datasets showed that the miR-1301-3p level was downregulated in PC tissues compared with that in adjacent healthy tissues. Furthermore, low expression of miR-1301-3p correlated with unsatisfactory outcomes and malignant phenotypes. Therefore, our observations supported that miR-1301-3p may serve as a prognostic biomarker for PC. Further experiments revealed that miR-1301-3p inhibits the proliferation, migration, and invasion abilities of PC cells via RhoA induced EMT process.

RhoA is a member of the Rho GTPase family, containing a GTP-bound active form and a GDP inactive part^[16, 17]. As a small GTPase, RhoA plays a critical role in regulating actin organization and cell migration^[18]. However, the abnormal activation of the RhoA/ROCK1 pathway can promote carcinogenesis in many human cancers. Zhu et al. revealed that diindolylmethane could reverse EMT process and inhibit esophagus cancer metastasis through repressing RhoA/ROCK1 mediated COX2/PGE

pathway^[19]. In lung cancer, KRAS promoted cell metastasis via activating RhoA expression^[20]. Previous studies also pointed out that miRNAs regulated RhoA expression in multiple cancers^[21, 22]. For example, Fan et al. demonstrated that miR-154-3p and miR-487-3p specifically repressed RhoA expression at the post-transcriptional level in thyroid cancer^[23]. Furthermore, miR-101 negatively regulated EMT and migration capacity of cancer cells by directly reducing the RhoA level^[24].

A critical step of tumor metastasis is known as EMT process, in which cancer cells lose their polarities and cellular connections and acquire migration ability^{[25] [26]}. The EMT is characterized by loss of the cell-adhesion protein, E-cadherin and upregulation of N-cadherin and vimentin, representing mesenchymal phenotypes. It has been proven that EMT-activators promote tumor development in multiple human cancers^[27-30]. Activation of RhoA/ROCK signaling pathway may upregulate EMT process. For example, RhoA inhibition increased E-cadherin expression and suppressed proliferation and migration of lung cancer cells^[31]. RND1, a member of Rho GTPases, functioned as an anti-metastasis target via suppressing RhoA pathway in hepatocellular carcinoma^[32]. Also, Zhu et al. reported that ASIC1 and ASIC3 contributed to acidity-induced EMT of pancreatic cancer through activating Ca²⁺/RhoA pathway^[33]. In the current study, we demonstrate that miR-1301-3p can directly suppress RhoA induced EMT process in PC, and consequently, this miRNA may serve as a therapeutic target for PC metastasis.

Conclusion

In summary, we revealed that miR-1301-3p could serve as a prognostic biomarker for PC. Overexpression of miR-1301-3p inhibits PC cell proliferation, migration, and invasion. Mechanistically, miR-1301-3p suppresses RhoA induced EMT process, and thus, miR-1301-3p/RhoA could be a novel target for PC treatment.

Declarations

ACKNOWLEDGMENTS

We thank Drs. Hua Fan, Xianliang Li, Yu Liu, and Lixin Li for general support and providing samples.

AUTHOR CONTRIBUTIONS

The conception and design of the study, as well as manuscript writing were performed by Xinxue Zhang and Xin Zhao; administrative support was provided by Qiang He; the provision of study materials was by Ren Lang; the collection and assembly of data were by Jun Ma and Jiantao Kou; the experiments were performed by Zhe Liu and Junming Xu. All authors read and approved the final manuscript.

ADDITIONAL INFORMATION

Ethics approval and consent to participate The Research Ethics Committee of Beijing Chao-Yang Hospital affiliated to Capital Medical University approved the use of anonymized human pancreatic cancer

samples.

Availability of data and materials Not applicable.

Competing Interests The authors disclose no potential conflicts of interest.

Funding This work was supported by the Beijing Municipal Science & Technology Commission, PR China [Z181100001718164] and Capital's Funds for Health Improvement and Research, Beijing, PR China [CFH 2020-2-2036].

References

1. Siegel R, Ma J, Zou Z, Jemal A. Cancer statistics, 2014. *CA Cancer J Clin.* 2014; 64(1):9-29. doi.org/10.3322/caac.21208.
2. Vincent A, Herman J, Schulick R, Hruban RH, Goggins M. Pancreatic cancer. *Lancet.* 2011; 378(9791):607-620. doi.org/10.1016/S0140-6736(10)62307-0.
3. Zhang J, He J, Zhang L. The down-regulation of microRNA-137 contributes to the up-regulation of retinoblastoma cell proliferation and invasion by regulating COX-2/PGE2 signaling. *Biomed Pharmacother.* 2018; 106(35-42). doi.org/10.1016/j.biopha.2018.06.099.
4. Otto T, Candido SV, Pilarz MS, Sicinska E, Bronson RT, Bowden M, Lachowicz IA, Mulry K, Fassl A, Han RC, Jecrois ES, Sicinski P. Cell cycle-targeting microRNAs promote differentiation by enforcing cell-cycle exit. *Proc Natl Acad Sci U S A.* 2017; 114(40):10660-10665. doi.org/10.1073/pnas.1702914114.
5. Zhu L, Xue F, Xu X, Xu J, Hu S, Liu S, Cui Y, Gao C. MicroRNA-198 inhibition of HGF/c-MET signaling pathway overcomes resistance to radiotherapy and induces apoptosis in human non-small-cell lung cancer. *J Cell Biochem.* 2018; 119(9):7873-7886. doi.org/10.1002/jcb.27204.
6. Alidadiani N, Ghaderi S, Dilaver N, Bakhshamin S, Bayat M. Epithelial mesenchymal transition Transcription Factor (TF): The structure, function and microRNA feedback loop. *Gene.* 2018; 674(115-120). doi.org/10.1016/j.gene.2018.06.049.
7. Peng X, Yan B, Shen Y. MiR-1301-3p inhibits human breast cancer cell proliferation by regulating cell cycle progression and apoptosis through directly targeting ICT1. *Breast Cancer.* 2018; 25(6):742-752. doi.org/10.1007/s12282-018-0881-5.
8. Zhi T, Jiang K, Zhang C, Xu X, Wu W, Nie E, Yu T, Zhou X, Bao Z, Jin X, Zhang J, Wang Y, Liu N. MicroRNA-1301 inhibits proliferation of human glioma cells by directly targeting N-Ras. *Am J Cancer Res.* 2017; 7(4):982-998.
9. Zhang Z, Pan B, Lv S, Ji Z, Wu Q, Lang R, He Q, Zhao X. Integrating MicroRNA Expression Profiling Studies to Systematically Evaluate the Diagnostic Value of MicroRNAs in Pancreatic Cancer and Validate Their Prognostic Significance with the Cancer Genome Atlas Data. *Cell Physiol Biochem.* 2018; 49(2):678-695. doi.org/10.1159/000493033.

10. Yu G, Wang LG, Han Y, He QY. clusterProfiler: an R package for comparing biological themes among gene clusters. *OMICS*. 2012; 16(5):284-287. doi.org/10.1089/omi.2011.0118.
11. Wang B, Wu H, Chai C, Lewis J, Pichiorri F, Eisenstat DD, Pomeroy SL, Leng RP. MicroRNA-1301 suppresses tumor cell migration and invasion by targeting the p53/UBE4B pathway in multiple human cancer cells. *Cancer Lett*. 2017; 401(20-32). doi.org/10.1016/j.canlet.2017.04.038.
12. Yang C, Xu Y, Cheng F, Hu Y, Yang S, Rao J, Wang X. miR-1301 inhibits hepatocellular carcinoma cell migration, invasion, and angiogenesis by decreasing Wnt/beta-catenin signaling through targeting BCL9. *Cell Death Dis*. 2017; 8(8):e2999. doi.org/10.1038/cddis.2017.356.
13. Liu Y, Wu G. NNT-AS1 enhances bladder cancer cell growth by targeting miR-1301-3p/PODXL axis and activating Wnt pathway. *NeuroUrol Urodyn*. 2020; 39(2):547-557. doi.org/10.1002/nau.24238.
14. Wen J, Wang H, Dong T, Gan P, Fang H, Wu S, Li J, Zhang Y, Du R, Zhu Q. STAT3-induced upregulation of lncRNA ABHD11-AS1 promotes tumour progression in papillary thyroid carcinoma by regulating miR-1301-3p/STAT3 axis and PI3K/AKT signalling pathway. *Cell Prolif*. 2019; 52(2):e12569. doi.org/10.1111/cpr.12569.
15. Huang H, Bu YZ, Zhang XY, Liu J, Zhu LY, Fang Y. LINC01433 promotes hepatocellular carcinoma progression via modulating the miR-1301/STAT3 axis. *J Cell Physiol*. 2019; 234(5):6116-6124. doi.org/10.1002/jcp.27366.
16. Itoh K, Yoshioka K, Akedo H, Uehata M, Ishizaki T, Narumiya S. An essential part for Rho-associated kinase in the transcellular invasion of tumor cells. *Nat Med*. 1999; 5(2):221-225. doi.org/10.1038/5587.
17. Sahai E, Marshall CJ. RHO-GTPases and cancer. *Nat Rev Cancer*. 2002; 2(2):133-142. doi.org/10.1038/nrc725.
18. Hodge RG, Schaefer A, Howard SV, Der CJ. RAS and RHO family GTPase mutations in cancer: twin sons of different mothers? *Crit Rev Biochem Mol Biol*. 2020; 55(4):386-407. doi.org/10.1080/10409238.2020.1810622.
19. Zhu P, Yu H, Zhou K, Bai Y, Qi R, Zhang S. 3,3'-Diindolylmethane modulates aryl hydrocarbon receptor of esophageal squamous cell carcinoma to reverse epithelial-mesenchymal transition through repressing RhoA/ROCK1-mediated COX2/PGE2 pathway. *J Exp Clin Cancer Res*. 2020; 39(1):113. doi.org/10.1186/s13046-020-01618-7.
20. Hung PS, Huang MH, Kuo YY, Yang JC. The Inhibition of Wnt Restrain KRAS(G12V)-Driven Metastasis in Non-Small-Cell Lung Cancer. *Cancers (Basel)*. 2020; 12(4). doi.org/10.3390/cancers12040837.
21. Dopeso H, Rodrigues P, Bilic J, Bazzocco S, Carton-Garcia F, Macaya I, de Marcondes PG, Anguita E, Masanas M, Jimenez-Flores LM, Martinez-Barriocanal A, Nieto R, Segura MF. et al. Mechanisms of inactivation of the tumour suppressor gene RHOA in colorectal cancer. *Br J Cancer*. 2018; 118(1):106-116. doi.org/10.1038/bjc.2017.420.
22. Ge F, Wang C, Wang W, Liu W, Wu B. MicroRNA-31 inhibits tumor invasion and metastasis by targeting RhoA in human gastric cancer. *Oncol Rep*. 2017; 38(2):1133-1139. doi.org/10.3892/or.2017.5758.

23. Fan XD, Luo Y, Wang J, An N.miR-154-3p and miR-487-3p synergistically modulate RHOA signaling in the carcinogenesis of thyroid cancer. *Biosci Rep.* 2020; 40(1). doi.org/10.1042/BSR20193158.
24. Chandra Mangalhari K, Manvati S, Saini SK, Ponnusamy K, Agarwal G, Abraham SK, Bamezai RNK.ERK2-ZEB1-miR-101-1 axis contributes to epithelial-mesenchymal transition and cell migration in cancer. *Cancer Lett.* 2017; 391(59-73). doi.org/10.1016/j.canlet.2017.01.016.
25. Das V, Bhattacharya S, Chikkaputtaiah C, Hazra S, Pal M.The basics of epithelial-mesenchymal transition (EMT): A study from a structure, dynamics, and functional perspective. *J Cell Physiol.* 2019. doi.org/10.1002/jcp.28160.
26. Kalluri R, Weinberg RA.The basics of epithelial-mesenchymal transition. *J Clin Invest.* 2009; 119(6):1420-1428. doi.org/10.1172/JCI39104.
27. Canel M, Serrels A, Frame MC, Brunton VG.E-cadherin-integrin crosstalk in cancer invasion and metastasis. *J Cell Sci.* 2013; 126(Pt 2):393-401. doi.org/10.1242/jcs.100115.
28. Labernadie A, Kato T, Brugues A, Serra-Picamal X, Derzsi S, Arwert E, Weston A, Gonzalez-Tarrago V, Elosegui-Artola A, Albertazzi L, Alcaraz J, Roca-Cusachs P, Sahai E.et al.A mechanically active heterotypic E-cadherin/N-cadherin adhesion enables fibroblasts to drive cancer cell invasion. *Nat Cell Biol.* 2017; 19(3):224-237. doi.org/10.1038/ncb3478.
29. Richardson AM, Havel LS, Koyen AE, Konen JM, Shupe J, Wiles WGt, Martin WD, Grossniklaus HE, Sica G, Gilbert-Ross M, Marcus AI.Vimentin Is Required for Lung Adenocarcinoma Metastasis via Heterotypic Tumor Cell-Cancer-Associated Fibroblast Interactions during Collective Invasion. *Clin Cancer Res.* 2018; 24(2):420-432. doi.org/10.1158/1078-0432.CCR-17-1776.
30. Padmanaban V, Krol I, Suhail Y, Szczerba BM, Aceto N, Bader JS, Ewald AJ.E-cadherin is required for metastasis in multiple models of breast cancer. *Nature.* 2019; 573(7774):439-444. doi.org/10.1038/s41586-019-1526-3.
31. Asnaghi L, Vass WC, Quadri R, Day PM, Qian X, Braverman R, Papageorge AG, Lowy DR.E-cadherin negatively regulates neoplastic growth in non-small cell lung cancer: role of Rho GTPases. *Oncogene.* 2010; 29(19):2760-2771. doi.org/10.1038/onc.2010.39.
32. Qin CD, Ma DN, Zhang SZ, Zhang N, Ren ZG, Zhu XD, Jia QA, Chai ZT, Wang CH, Sun HC, Tang ZY.The Rho GTPase Rnd1 inhibits epithelial-mesenchymal transition in hepatocellular carcinoma and is a favorable anti-metastasis target. *Cell Death Dis.* 2018; 9(5):486. doi.org/10.1038/s41419-018-0517-x.
33. Zhu S, Zhou HY, Deng SC, Deng SJ, He C, Li X, Chen JY, Jin Y, Hu ZL, Wang F, Wang CY, Zhao G.ASIC1 and ASIC3 contribute to acidity-induced EMT of pancreatic cancer through activating Ca(2+)/RhoA pathway. *Cell Death Dis.* 2017; 8(5):e2806. doi.org/10.1038/cddis.2017.189.

Figures

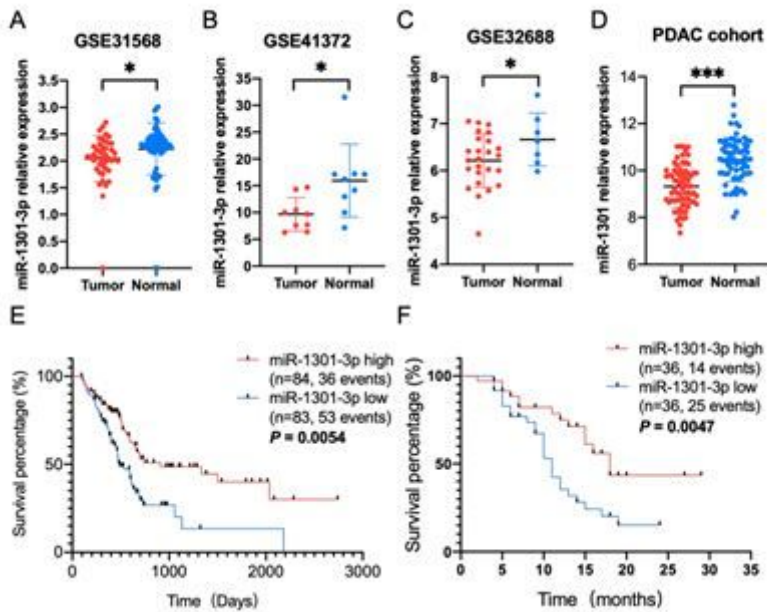


Figure 1

MiR-1301-3p was expressed at low levels in pancreatic cancer (PC), relating to a good prognosis for PC patients. A-C. In GSE31568, GSE41372, and GSE32688, miR-1301-3p expression level was significantly lower in PC than in healthy tissues. D. In PC tissues, miR-1301-3p was also downregulated following qRT-PCR detection. E and F. In the PC cohort of the TCGA and the validation cohort, a high level of miR-1301-3p was associated with long overall survival for PC patients. * $p < 0.05$, *** $p < 0.001$.

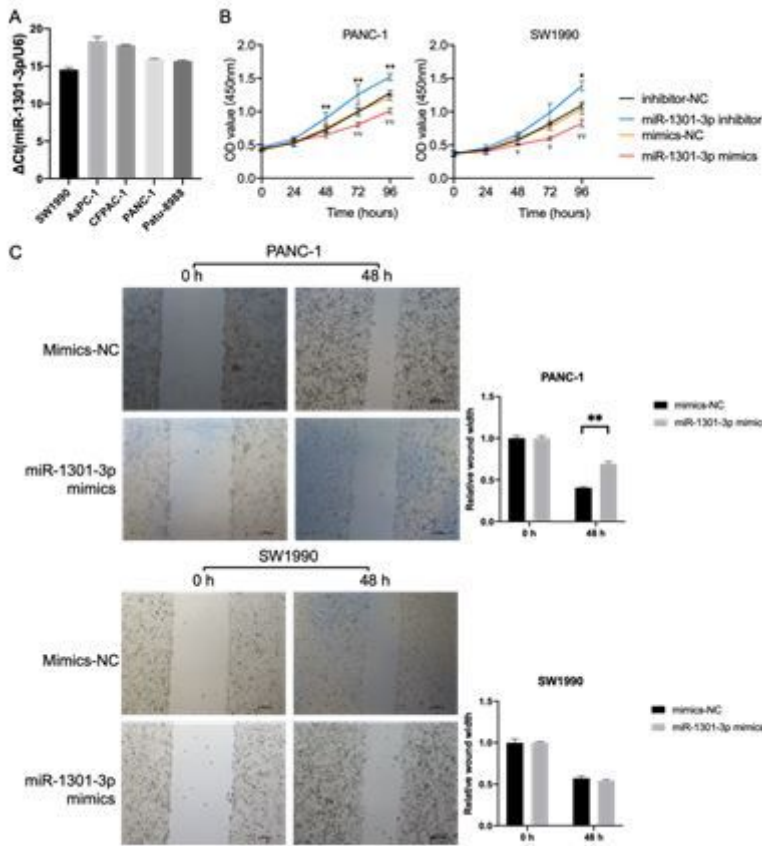


Figure 2

MiR-1301-3p inhibited the proliferation and migration ability of PC cells. A. Relative expression of miR-1301-3p in five PC cell lines. B. CCK-8 assays showed that miR-1301-3p significantly repressed PC cell proliferation ability C. The wound healing assays suggested that miR-1301-3p negatively regulated PANC-1 cell migration, but it failed to affect SW1990 cell metastasis. * $p < 0.05$, ** $p < 0.01$, $\nabla p < 0.05$, $\nabla\nabla p < 0.01$.

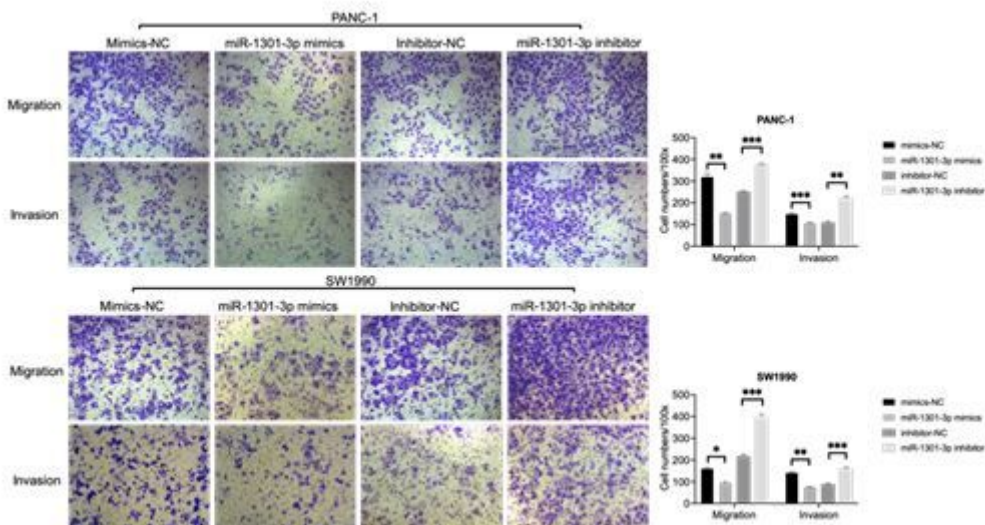


Figure 3

MiR-1301-3p suppressed PC cell invasion. Transwell assays showed that miR-1301-3p inhibited the migration and invasion ability in PANC-1 and SW1990 cells. * $p < 0.05$, ** $p < 0.01$, *** $p < 0.001$.

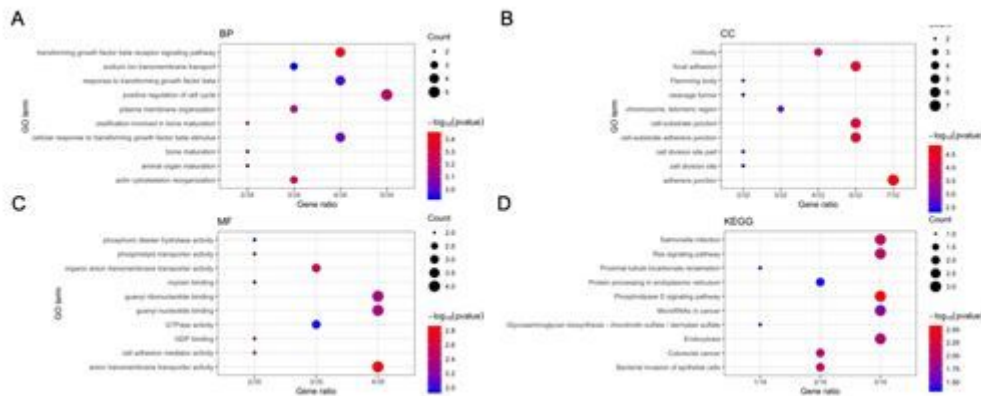


Figure 4

Functional annotation and pathway enrichment for miR-1301-3p. A-C. Gene Ontology analyses, including biological process, cellular component, and molecular function. D. Kyoto Encyclopedia of Gene and Genomes pathway enrichment.

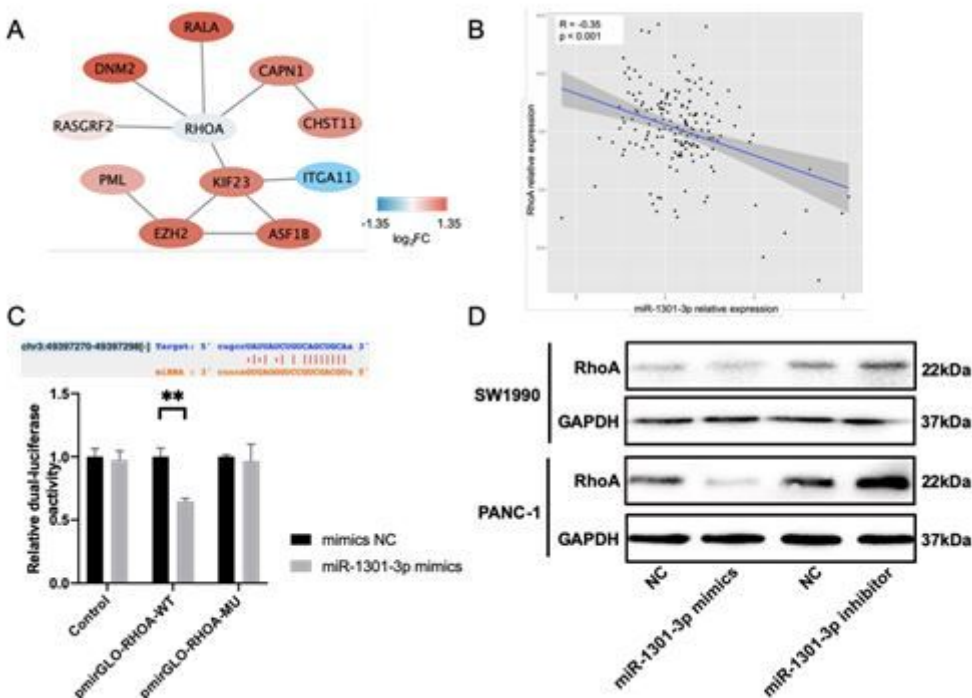


Figure 5

MiR-1301-3p directly targeted RhoA. A. A protein-protein interaction network identified that RhoA possibly acted as a central gene among the hub genes of miR-1301-3p. B. A negative correlation between miR-

1301-3p and RhoA expressions. C. Luciferase reporter assays demonstrated that miR-1301-3p directly bound to 3'UTR of RhoA. D. Western blotting assays suggested that miR-1301-3p downregulated RhoA protein expression in PC cells.

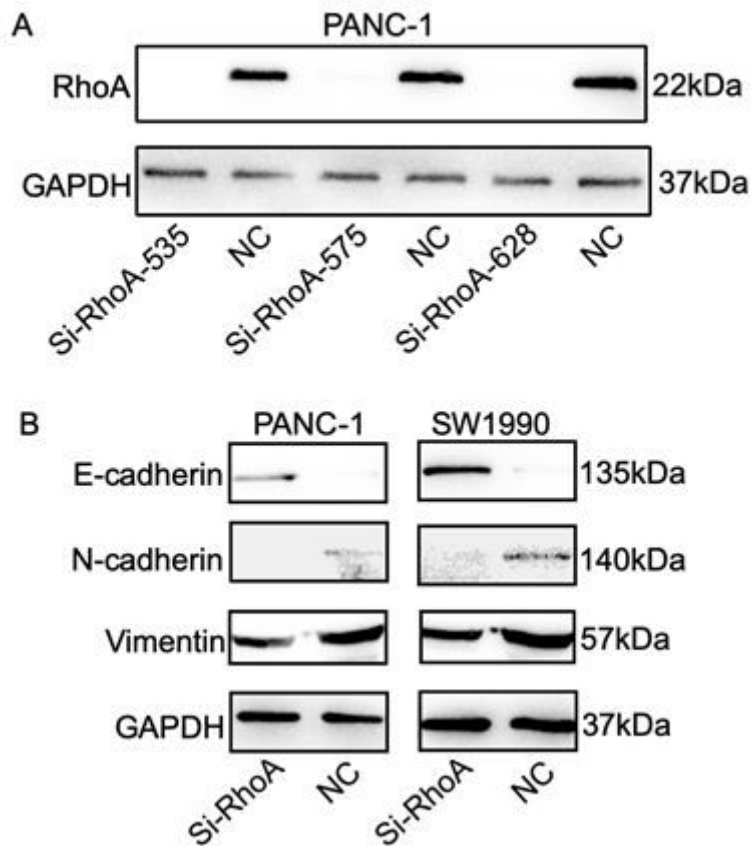


Figure 6

RhoA knockdown inhibited the epithelial-mesenchymal transition process in PC cells. A. Three small interference RNAs against RhoA (Si-RhoA) significantly separately suppressed RhoA expression. B. Western blotting assays showed that knockdown of RhoA upregulated E-cadherin expression; however, downregulated N-cadherin and vimentin levels.